Disintegration of Helium by 90-Mev Neutrons

PETER E. TANNENWALD*
Radiation Laboratory, Department of Physics, University of California, Berkeley, California
(Received August 11, 1952)

A detailed study of the fragments produced from helium when bombarded by 90-Mev neutrons was made in a 22-inch cloud chamber filled with helium gas and operated in a pulsed magnetic field of 22 000 gauss. The particles were identified by curvature and relative ionization, or by change of curvature with range when they stopped in the chamber. The energy of the incident neutron could be calculated from measured quantities for most modes of disintegration. The total number of events, for incident neutrons above 40 Mev, was normalized to the interpolated n-He^4 total cross section of 1.9×10^{-25} cm^2; thus absolute cross sections were established for the various disintegration processes. Energy dependences were compared and energy and angular distributions have been determined.

I. INTRODUCTION

NUCLEON–NUCLEON scattering provides one of the most direct ways of gaining information about the forces between nucleons. Yet the scattering and disintegration of nuclei by nucleons has been a most fruitful approach in establishing various models of the nucleus and in revealing the behavior of large numbers of nucleons in close proximity. The disintegration of helium presents a unique case in that there are so few particles that a theoretical analysis of the interactions between individual nucleons can be hoped for; and on the other hand, due to the tightly bound structure of helium, it will show some of the properties of heavier nuclei. If it is true, as is sometimes believed, that the alpha-particle exists as a sub-structure in heavier nuclei, then the disintegration of helium will be of value in interpreting the disintegrations of heavier nuclei.

The charged particles ejected from nuclei when bombarded by 90-Mev neutrons have been studied in a number of experiments,[1] and the results indicate that the nature of the collision process for high energies is determined predominantly by the interaction of the bombarding particle with an individual nucleon rather than with the struck nucleus as a whole.

Neutron-induced stars are especially suited for study in a cloud chamber. In the first star experiment using 90-Mev neutrons, Tracy and Powell[2] filled their chamber with a mixture of oxygen and helium gas. In the present investigation a more complete analysis was possible due to the use of helium gas alone in the chamber, a more powerful magnetic field,[3] and experience with neutron-deuteron scattering.[4]

II. EXPERIMENTAL PROCEDURE

The 90-Mev neutrons produced in the stripping process by bombarding a 2-inch thick beryllium target with 190-Mev deuterons were collimated outside the concrete shielding of the 184-inch Berkeley cyclotron by means of a rectangular copper collimator four feet long passing a beam $2\frac{3}{4}$ in. wide and $\frac{3}{4}$ in. high (see Fig. 1). The neutrons were then allowed to enter a 22-inch Wilson cloud chamber[3] through a 3×1 inch aluminum foil 1 mil thick, and to pass out through a similar window in order to reduce backscattering from the rear wall of the chamber.

The cloud chamber was operated in a pulsed magnetic field of 22 000 gauss. The cycle of operations, which was repeated once a minute, was as follows: the current through the magnet is turned on in advance so that its maximum coincides with the expansion of the chamber. The cyclotron beam is pulsed through the chamber at the instant the moving diaphragm of the chamber hits the bottom, and the lights are flashed 0.03 sec later.

The chamber was filled with 99 percent pure helium gas to a total pressure of 81.5 cm Hg; in the expanded equilibrium position 1.8 cm of this pressure was due to the partial water vapor pressure from the moist gelatine covering the diaphragm. Immediately after expansion the ration of helium to oxygen nuclei was 51.8. The expansion ratio during the experiment was approximately 17 percent.

The pictures were taken by a twin-lens camera and reprojected to natural size through the same lenses in a stereo-projector.[5] (See Fig. 2.)

III. METHOD OF ANALYSIS OF EVENTS

On the average, three two-prong stars and about an equal number of heavily-ionizing single tracks appear in each picture. The possible reactions when a neutron strikes a helium nucleus are as follows:

Inelastic	$n+He^4\rightarrow d+t$	(dt)
	$\rightarrow p+t+n$	(pt)
	$\rightarrow d+d+n$	(dd)
	$\rightarrow p+d+2n$	(pd)
	$\rightarrow p+p+3n$	(pp)
	$\rightarrow He^3+2n$	(He^3)
Elastic	$\rightarrow He^4+n$	(He^4)

* Present address: Project Lincoln, Massachusetts Institute of Technology, Cambridge, Massachusetts.

[1] K. Brueckner and W. Powell, Phys. Rev. **75**, 1274 (1949); and J. Hadley and H. F. York, Phys. Rev. **80**, 345 (1950).

[2] J. Tracy and W. Powell, Phys. Rev. **77**, 594 (1950).

[3] W. Powell, Rev. Sci. Instr. **20**, 402 (1949).

[4] W. Powell (to be published). See also University of California Radiation Laboratory Report UCRL-1191.

[5] Brueckner, Hartsough, Hayward, and Powell, Phys. Rev. **75**, 555 (1949).

Analysis of an event involving the helium nucleus requires identification of protons, deuterons, tritons, He^3 nuclei, and He^4 nuclei. Stars with three or more prongs are observed occasionally; they are due to oxygen nuclei in the water vapor. The identification of the particles involved in the two-prong stars rests mainly on measurement of their radii of curvature and an estimate of their relative ionizations. If one knows the strength of the magnetic field at the position of the tracks, two out of the following three quantities determine the third: curvature, ionization, particle identity.

Two-Prong Stars

A two-prong star from helium can only include singly charged particles, and over the range of energies observed in this experiment, a simple rule holds. For a given radius of curvature the ionization of a deuteron is approximately three times that produced by a proton and of a triton is six times that for a proton. A table was constructed which gives $H\rho$ *vs* ionization for p, d, t, He^3, and He^4, and it is used in the following way.

In each picture a more or less parallel beam of lightly ionizing particles can be seen to come through the entrance window with radii around 35 cm. The fact that the ionization of these tracks is the lightest observed for these curvatures plus the fact that occasionally tracks are observed to come in with these curvatures which appear denser but never lighter, establishes these background tracks as protons. This verifies the expectation that protons are knocked out of the walls of the collimator and window by the incident neutrons. Since their identities and curvatures are established, their ionizations can be obtained from the table, and thus a starting point has been made in finding reference ionizations. Furthermore if the ionization of a track from helium falls in the proper range, it can be bracketed between two background proton tracks.

Various other aids can be employed in identifying particles. If, for example, one prong of a star is a deuteron and the two prongs are not coplanar with the neutron beam direction, then it is very unlikely that the other prong is a triton. Or, one prong may end in the chamber giving rise to a characteristic ending. A unique

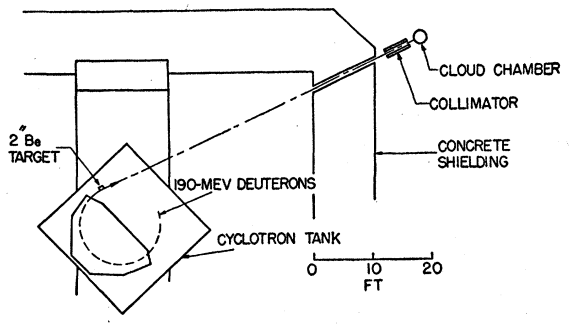

FIG. 1. Sketch of cyclotron, cloud chamber, and collimation arrangement.

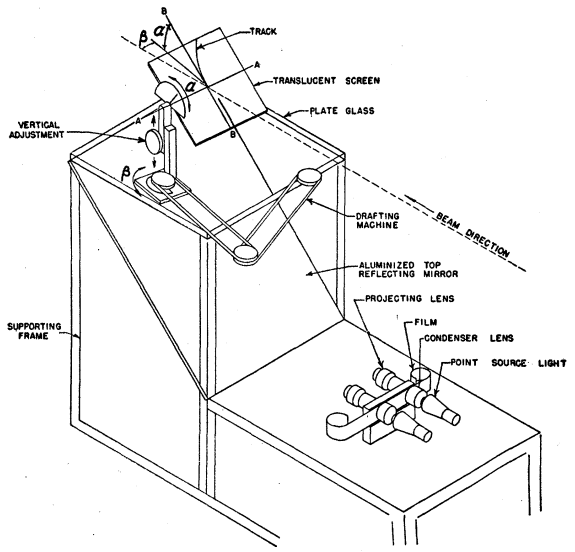

FIG. 2. Stereo-projector used to reproject events to natural size. Dip angle α and beam angle β are indicated.

theoretical relation exists for each particle which relates $H\rho$ *vs* residual range, and the ending of the track in question can be compared with the theoretically computed track shape or with an experimental characteristic ending in the same gas mixture which has previously been well established from other evidence.

By such reference and bracketing procedures it has been possible to identify the fragments from two-prong stars in most cases. Out of 179 two-prong stars whose tracks lay within angles of $\pm 30°$ to the horizontal plane, eight could not be analyzed with certainty. Of these eight, four had one or both prongs too short, and four were either pd's or pt's. The latter uncertainty stems from the fact that when a track has an ionization with respect to minimum starting at about 70 times minimum, it is very difficult to decide whether the ionization is 70 times or twice as great.

Single-Prong Stars

The single tracks from helium are He^3's and He^4 recoils. These tracks turn out to be most frequently of low energy and they will then be extremely heavy and often also short. Ionizations fall in the range above 100 where estimates of density are not sufficiently accurate to distinguish between He^3 and He^4. However, if the track stops in the chamber, it can be compared with a characteristic ending; if it does not stop in the chamber, the change in curvature along the track is insufficient to determine whether it is He^3 or He^4.

Figures 3 and 4 show some representative stars and characteristic endings.

Measurements

The technique used in reprojecting the events and the whole question of accuracy of measurements have been discussed by Powell and associates.[4]

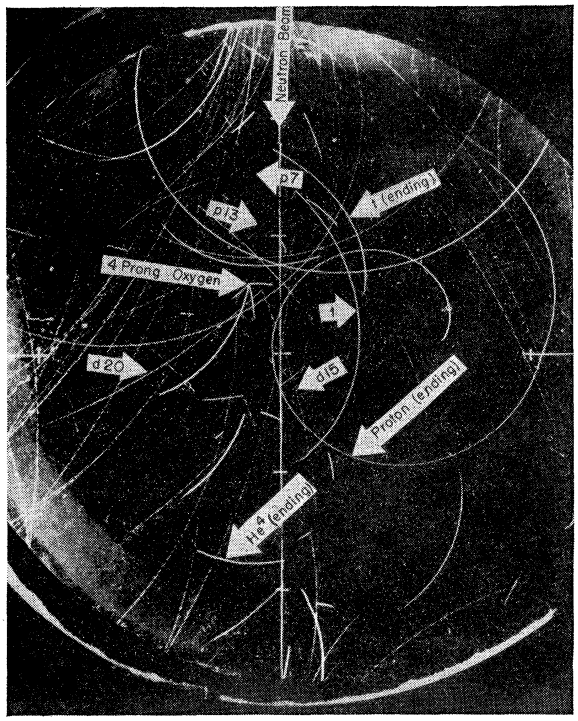

FIG. 3. Photograph showing examples of events that were analyzed. The letters are abbreviations for the particles and the numbers stand for the dE/dx values with respect to minimum ionization.

All angular measurements rest on the assumption that the incident neutrons entered the chamber in a parallel beam. This assumption is verified by the fact that the number of stars produced outside the volume swept out by the neutron beam is negligible.

In the present experiment complete analysis of stars was limited to those events which had all their prongs lying within dip angles of less than $\pm 30°$. (Dip angle is the angle between the initial track direction and its projection on the horizontal plane containing the neutron beam.) This restriction is necessary because when the prong under consideration is too slanted, accurate measurement of curvature and dip angle is impossible in a large number of cases. A very slanted track is usually short because it passes quickly out of the lighted region, and the extreme stereoscopic effect required of the lenses makes the superposition of the two images insensitive to variations of the slant plane. Imposition of this restriction necessitated an extended correction procedure, which is discussed below.

Calculations

The energy of the incident neutron causing a particular event can be calculated for most cases. Since the disintegration of helium by a neutron into a deuteron and triton is a two-body problem, the incident neutron energy can be calculated in two ways—momentum balance and energy conservation. In the case of *pt* and *dd* disintegrations, in which one secondary neutron comes off, it is still possible to calculate the energy of the incident neutron. But for *pd* events, in which two neutrons come off in addition to the proton and deuteron, only a minimum incident neutron energy can be computed if the two ejected neutrons are lumped together and treated as one particle with two neutron mass units with the requisite momentum to balance the problem.

In the elastic scattering cases, the measured energy of a He^4 recoil leads directly to the energy of the incident neutron, and the corresponding scatter angle of the neutron is independent of the particular He^4 recoil energy.

IV. CORRECTIONS

Single-Prong Stars

Only those events have been measured whose tracks lay within an angle of $\pm 30°$ to the horizontal plane. In order to find the number of events which would have been observed without this restriction on the dip angle, a weighting factor has to be assigned to each event. This factor is the reciprocal of the fraction of total solid angle available to the track if one uses the assumption of isotropic azimuthal distribution about the neutron beam direction. The appropriate correction factor was applied to each track individually. (See Appendix I for details.)

Two-Prong Stars

In the case of events with two prongs the correction procedure is complicated by the fact that the rejection of an event may be due to one or both prongs lying outside the $\pm 30°$ limit; and, furthermore, the fraction of total solid angle available to the event depends on the difference in azimuthal angles of the two tracks. The appropriate correction factor was applied to each event individually. (See Appendix I for details.)

As a check on this computed correction procedure, the events for which one or both prongs lay outside the $\pm 30°$ limit have been counted, and whenever possible, identified. The total number of these partially analyzed stars plus the total number of completely analyzed stars should be equal, within statistical errors, to the number of completely analyzed stars corrected by the computed solid angle correction. Such a check would also assure one that nothing significant was overlooked by confining α to less than $\pm 30°$. Certain few two-

TABLE I. Results of inelastic events.

	pt	*dt*	*pd*	*dd*	*pp*	He^3	Total
1. Measured	88.0	33.0	31.0	17.0	2.0		171.0
2. Not identified	5.1	0.8	1.7	0.4			8.0
3. Sum	93.1	33.8	32.7	17.4	2.0		179.0
4. Corrected total	212.6	75.5	76.3	37.0	3.8		
5. Total with He^3 assumption	212.6	75.5	76.3	37.0	3.8	83.5	488.7
6. Total for neutrons >40 Mev	209.1	66.5	76.3	35.2	3.8	80.8	471.7
7. Probable error	7.3%	12.3%	12.1%	16.8%	48.0%		5.2%

prong stars are conceivable where both prongs would never fall inside the 30° limits regardless of how the configuration was rotated about the beam axis. This situation would amount to an infinite computed solid angle correction factor, but it will be shown from the data that no significant contributions could have come from this type of star.

The He^3 Assumption

As has been mentioned before, it was impossible to determine whether a single track was He^3 or He^4 when it did not end in the chamber. In order to estimate what fraction of all the single tracks was He^3's, some assumption must be made regarding the He^3 formation mechanism.

The *pt* and He^3 events can be considered as similar processes—in one case the incoming neutron interacts with and strips a proton off the helium nucleus, while in the second case it strips off a neutron. As a simple approximation, it seems reasonable to expect the ratio of He^3 to *pt* events to be the same as the ratio of the free $n-n$ to the $n-p$ cross section at 90 Mev. To the extent of present knowledge, the numerical value of σ_{pp} must be employed for σ_{nn}; then the ratio becomes about $\frac{1}{3}$.[6]

Furthermore, those cases of the *dt* events in which a pick-up deuteron comes off in the forward direction must be included as a type of *pt* event because the deuteron is actually not formed until some time after the disintegration.[7] The number of He^3's is thus estimated to be

$$\tfrac{1}{3}\,[\text{No. of } pt \text{ events} + \text{pick-up } dt \text{ events}].$$

V. RESULTS AND DISCUSSION

1. Inelastic Events

The first row in Table I shows the inelastic events which had dip angles less than ±30° and were thus subject to a detailed analysis. In addition there were four stars which could not be identified and four stars where the interpretation could have been either *pd*'s or *pt*'s. These eight unidentified events were arbitrarily divided into groups with the same relative distribution as the identified events in the first row. The numbers in the second row show the grouping of these eight events.

Line 3 is the sum of line 1 and line 2. The fourth row gives the total number of events of each type which would have been observed if α had not been restricted to less than ±30°.

The fifth row shows the total number of inelastic events of each type including 83.5 events for He^3 obtained by using the assumption made in the section on Corrections. Row 6 is the same as row 5 except it includes only events from neutrons above 40 Mev.

Line 7 gives the statistical probable error based on events actually analyzed from neutrons above 40 Mev.

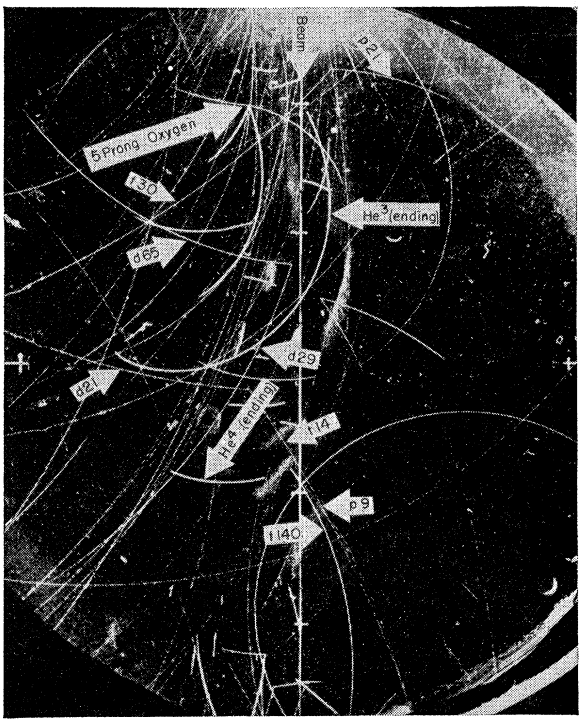

FIG. 4. Another sample picture. The lightest tracks which were dealt with are about 4–5 times with respect to minimum ionization and are only barely visible in the reproduction; the heaviest tracks encountered are as high as 400 times.

Results of Solid Angle Corrections

The following summarizes the evidence that no significant information was missed due to the fact that some stars might have had "unusual" configurations so as to have both prongs always outside the 30° limits:[8]

1. The number of events as computed from application of solid angle corrections to the analyzed stars in the 30° group is equal, within statistical error, to the number of counted (and partially analyzed) events outside the 30° limits. This proves that the number of "unusual" stars must be small.
2. The stars analyzed in the 30° group yield a certain distribution as to type of event. Those stars that were successfully analyzed in the group having one or both prongs outside have the same distribution of events.
3. The remaining stars in the group having one or both prongs outside, with one or both prongs not identified, can be arranged so as to give this same distribution.

Hence one can conclude that it is highly unlikely that there is any considerable number of stars of an "unusual" character among the events of item (3) whose presence would change the distribution in item (2) by a significant amount.

[6] Estimated from Hadley, Kelley, Leith, Segrè, Wiegand, and York, Phys. Rev. **75**, 351 (1949); and Chamberlain, Segrè, and Wiegand, Phys. Rev. **83**, 923 (1951).

[7] G. Chew and M. Goldberger, Phys. Rev. **77**, 470 (1950).

[8] For details see P. E. Tannenwald, University of California Radiation Laboratory Report UCRL-1767.

TABLE II. Results of elastic events.

He^4's ending in the chamber	139
Single tracks not ending	125
He^3's ending	2
Tracks less than 2 cm long	105
Tracks counted, with $\alpha > \pm 30°$ (ending and not ending)	349
Computed solid angle correction to He^4's ending	218
Computed solid angle correction to tracks not ending	127
Weighted single prong events due to neutrons >40 Mev	441

2. Elastic Events

Table II shows the results of measurements of the single prong stars. One has to determine now the number of single tracks which would have been observed if all solid angles had been looked at and if no tracks had been missed because they were too short. In order to correct for the solid angle limitation, a proper weighting factor has been applied to each individual event—as explained in detail previously. The angular distribution of the scattered neutrons shows a lack of neutrons in the forward direction, which is due to the short range of the recoils. It is proposed to extrapolate the experimental spectrum to zero scatter angle according to a reasonable theoretical assumption as to the shape of the spectrum, and it will be shown that 124 He^4 events from neutrons above 40 Mev are contributed by this extrapolation.

If the total number of neutron-helium collisions is to be normalized to the total n-He^4 cross section as determined indirectly by carbon disk detectors, those helium collisions must be excluded which were due to neutrons not present in the total cross-section experiment beam. The carbon activation reaction has a threshold at 20 Mev, and the number of neutrons detected between 20 and 40 Mev is small because of the sharp drop of the activation curve near the threshold and the small number of neutrons in that part of the spectrum.[9] Hence no serious error is introduced if only helium events from neutrons above 40 Mev are included in the normalization. There are very few inelastic events from neutrons between 20 and 40 Mev (see Table I)—the thresholds range from 17.5 Mev to 25.9 Mev—and also it will be shown that it is not feasible to correct for missed short elastic recoils from neutrons below 40 Mev.

In order to examine the question of why only two He^3's were observed ending in the chamber, one can again consider the analogy between the He^3 and pt processes. It is found that while 23 percent of the tritons from pt events stop in the chamber, only 5 percent of the He^3's stop (the total number of He^3's being based on the He^3 assumption). The following reasons could account for this:

1. The number of He^3's was grossly over-estimated in the He^3 assumption.

2. The He^3 energy distribution might differ from the triton energy distribution such that no low energy He^3's are emitted. (They would have to have less than a few Mev in order to end in the chamber.)

3. The He^3 energy distribution might differ from the triton energy distribution such that most He^3's received very little energy. In this case the short tracks could be confused with He^4. It should also be noted that for a given energy the range of a He^3 is only about one-third that of a triton.

3. Cross Sections

In order to obtain absolute cross sections the total number of events (472 inelastic+484 elastic), for incident neutrons above 40 Mev, is normalized to the interpolated n-He^4 total cross section from the work of Cook *et al.*[9] When σ is plotted *vs* $A^{\frac{2}{3}}$ for H, D, Li, and Be, σ for He turns out to be 1.9×10^{-25} cm^2 when the points are connected by a smooth curve. A probable error of 10 percent is arbitrarily assigned to this value.

On the basis of the inelastic and elastic events listed, the results are: $\sigma_{\text{elastic}}=96\pm17$ mb; $\sigma_{pt}=42\pm6$ mb; $\sigma_{dt}=13\pm2.5$ mb; $\sigma_{pd}=15\pm2.5$ mb; $\sigma_{dd}=7\pm1.5$ mb; $\sigma_{pp}=0.8\pm0.4$ mb; $\sigma_{He^3}=16$ mb (assumed). The ratio $\sigma_{\text{inelastic}}/\sigma_{\text{total}}$ is 0.49 ± 0.07.

4. Errors

The errors quoted in Table I are the statistical probable errors based on the number of events actually analyzed. For each quantity making up the 484 elastic events a statistical probable error can be associated based on the number of events actually measured. But it is more realistic to consider the magnitude of the extrapolation that had to be made for missed tracks and the uncertainty in the 80.8 assumed He^3 events, and consequently a probable error of ±60 was assigned to the 484 recoils.

5. Comparison with Theory

In 1950 Heidmann published an analysis of the 90-Mev neutron-helium scattering problem;[10] it is interesting to compare his predictions for the relative cross sections with the present experimental findings (Table III[10,11]).

If Heidmann's revised theoretical results were diminished by the ratio 190 mb/244 mb so as to make his

TABLE III. Comparison of experiment with Heidmann's theory.

Process	Theory[a]	Theory revised[b]	Experiment
elastic He^4	180 mb	160 mb	96±17 mb
pt	63	60±10	42±6
dt	16	16	13±2.5
pd	~0	~2	15±2.5
dd	~0	~0	7±1.5
pp	~0	~0	0.8±0.4
He^3	6	~6	16 (assumed)

[a] See reference 10.
[b] See reference 11.

[9] Cook, McMillan, Peterson, and Sewell, Phys. Rev. **75**, 7 (1949).

[10] J. Heidmann, Phil. Mag. **41**, 444 (1950).
[11] J. Heidmann (private communication).

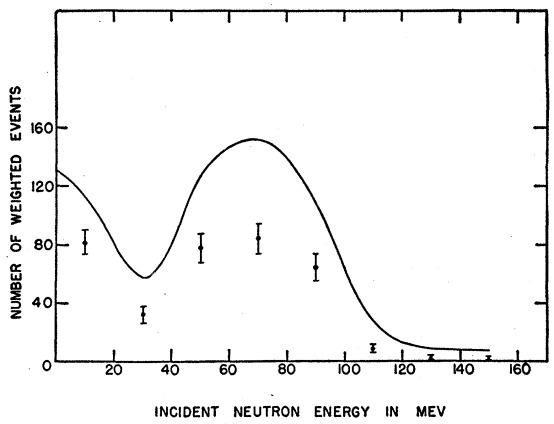

FIG. 5. Incident neutron spectrum weighted by the n-He elastic scattering cross section, as measured from He^4's ending in the chamber (single points), and as measured from all single prong events on the assumption that they are all He^4's (solid curve).

total cross section equal to the interpolated experimental value, the agreement would be excellent for the He^4, pt, and dt modes of disintegration. In any case the agreement is remarkable because, as the author himself points out, the calculations should be criticized for use of Gaussian functions for the potential and for the use of deuteron wave functions, which were employed to simplify the integrations. Heidmann apparently underestimates the occurrence of the pd and dd processes, but agrees that complete disintegration of helium by a neutron (pp) is rare.

In arriving at the number of He^3 disintegrations, Heidmann was the first to consider the pt and He^3 events as similar processes. However, he estimated that the ratio of He^3 to pt events would be given by

$$\frac{\frac{1}{4}}{\frac{1}{4}+\frac{3}{4}}\left(\frac{V\text{ singlet}}{V\text{ triplet}}\right)^2,$$

or about one-tenth. As discussed in the section on Corrections, in the present investigation the ratio of He^3 to pt events is assumed to be

$$\sigma_{nn}/\sigma_{np}=\sigma_{pp}/\sigma_{np}=\tfrac{1}{3},$$

which leads to about three times the He^3 cross section. Only the He^3 and He^4 cross sections and the ratio $\sigma_{\text{inelastic}}/\sigma_{\text{total}}$ are affected if one uses one or the other assumption. One piece of evidence which speaks in favor of the $\frac{1}{3}$ ratio comes from $n-d$ scattering at 90 Mev. Powell[4] found that the cross section for the production of protons with less than 10 Mev is 14.6 mb and that for protons with more than 10 Mev is 51.1 mb. The low energy protons are roughly isotropic and are left behind when the incident neutron hits the neutron in the deuteron, while the higher energy protons come off predominantly forward and result from the incident neutron striking the proton in the deuteron. The ratio between these two processes, which can be considered as n-n and n-p interactions in a light nucleus, is $\frac{1}{3}$.

6. Energy Dependence

The experimental information available is the incident neutron spectrum weighted by the n-He scattering cross section. In Fig. 5, the single points give this function as measured from He^4 recoils ending in the chamber. If all the single tracks which do not end in the chamber are included, the upper curve results. It is seen to have a quite similar shape, which is to be expected since the He^3's have been estimated to constitute only about 10 percent of the total spectrum. (Of course below 20.5 Mev the events must all be due to He^4 since this is the threshold for the He$^4(n, 2n)$He^3 reaction.) The peak occurs at about 70±5 Mev. The distribution has the general features resulting experimentally from the deuteron stripping process, namely a peak near half the deuteron energy and an apparent peak of low energy neutrons. Since both the energy dependence of elastic n-He scattering and the exact shape of the low energy end of the neutron spectrum are unknown, one cannot draw any conclusions as to the reality of the low energy neutron peak. The broadness of the spectrum and the shift of the main peak down to 70 Mev is due to the fact that the stripping target used in this part of the experiment was 2-inch Be rather than the more desirable $\frac{1}{2}$-inch Be.

For the various inelastic processes, the number of events *vs* incident neutron energy is plotted in Fig. 6; the peaks occur at about

pt: 75±5 Mev
di: 65±5 Mev
pd: 67±5 Mev.

(The neutron energy in the pd cases is a minimum.)

Since the incident neutron spectrum was the same in each case, the qualitative nature of the curves can be compared. The small shift of the pd curve to lower energies with respect to the pt curve may simply reflect the fact that the calculated value of the neutron energy gives a minimum only. The dt curve shows a decided energy dependence, and this agrees with the sharp falling off with energy of the pick-up process, which is

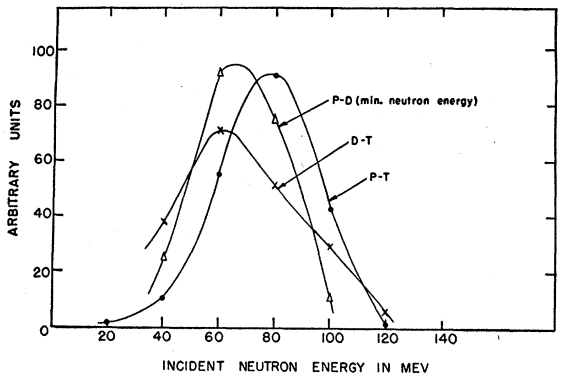

FIG. 6. Incident neutron spectrum weighted by n-He cross sections as measured from various inelastic events. Curves have been normalized to have the same area.

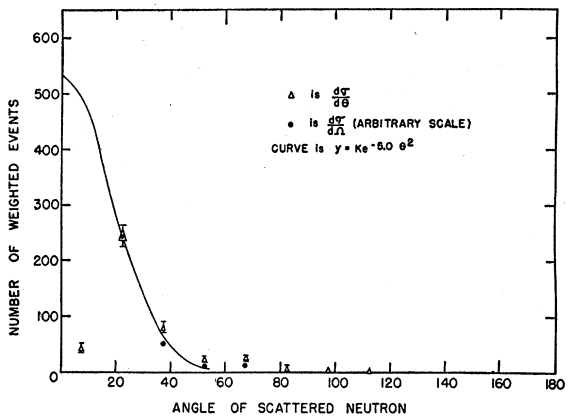

FIG. 7. Relative number of elastically scattered neutrons per unit scatter angle and per unit solid angle from incident neutrons above 40 Mev. Solid curve comes from theory.

theoretically expected. Preliminary experimental results on *n-d* pick-up deuterons verify this sharp energy dependence.[12]

7. Energy and Angular Distributions

Elastically Scattered Neutrons

The elastic events were divided into two groups—those due to incident neutrons below 40 Mev and those due to incident neutrons above 40 Mev. The reasons for this division are first that there exists evidence that low energy neutrons scatter from helium in a different manner than high energy neutrons;[13] second to be able to make a comparison with theory, in particular that due to Heidmann;[10] and third for a reason which will become evident in the next paragraphs.

The points denoted by triangles in Fig. 7 show the angular distribution of elastically scattered neutrons ($d\sigma/d\theta$) from incident neutrons with energies greater than 40 Mev; the points denoted by circles were obtained by dividing the $d\sigma/d\theta$ points by the average value of the sine over the 15° intervals and represent thus $d\sigma/d\Omega$. All single prongs not ending in the chamber have been included in this plot, but little error was made since only about 15 percent of the events above 40 Mev are estimated to be contributed by He^3's. Evidently there is a hole in the experimental distribution near the forward direction; it is due to the corresponding recoils being too short to be measured with certainty.

According to Heidmann's theory the angular distribution of 90 Mev elastically scattered neutrons is a Gaussian curve centered on the forward direction. His predicted curve has the equation

$$d\sigma/d\Omega = 4.50 \exp(-7.86\theta^2) \times 10^{-25} \text{ cm}^2$$

in the c.m. system. Since the present experimental data are consistent with a Gaussian, it was decided to draw a Gaussian curve through the experimental points; its form is

$$d\sigma/d\Omega = K \exp(-5.0\theta^2).$$

It is shown by the solid line in Fig. 7 and was extrapolated to zero degrees scatter angle.

Advantage has been taken previously of the opportunity to associate the events under the extrapolated part of the curve with the events missed because the tracks were too short. The reason why the angular distribution was plotted in 15° groups is that when a 40-Mev neutron is scattered at 15°, the corresponding recoil will just be 2 cm long. (This was the criterion selected below which recoils were merely counted instead of measured.) Consequently one begins to lose measurable tracks for neutron scatter angles of 15° and less. The critical alpha recoil angle corresponding to the neutron scatter angle of 15° is 80.5°. Recoils have been observed at angles as high as 84°; they are due to neutrons of energies higher than 40 Mev.

Figure 8 shows the angular distribution of elastically scattered neutrons from incident neutrons with energies less than 40 Mev. Here again a substantial number of neutrons are known to be missing near the forward direction. But since they can be missing up to fairly large neutron scatter angles (when a 5-Mev neutron is scattered at 45°, its alpha-recoil will just be 2 cm long), it is not possible to estimate the distribution of the missing tracks. However, the distribution confirms the general trend found by Swartz[13] that elastic scattering is peaked less in the forward direction at lower energies. The picture is qualitatively that the forward peak of diffraction scattering on the basis of the opaque nucleus model is spread out at lower energies, and that more nearly isotropic scattering is approached.

The $He^4(n, d)i$ *Reaction*

The angular distribution of deuterons from *dt* events is plotted in Fig. 9 and shows the expected peak of pick-up deuterons in the forward direction. The distribution is plotted both in terms of $d\sigma/d\theta$ and $d\sigma/d\Omega$.

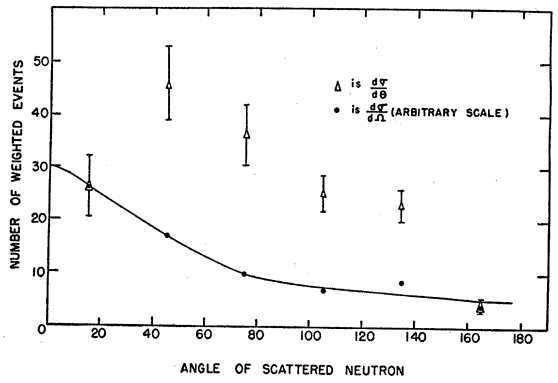

FIG. 8. Relative number of elastically scattered neutrons per unit scatter angle and per unit solid angle from incident neutrons below 40 Mev.

[12] A. Bratenahl (private communication).
[13] C. Swartz, Phys. Rev. **85**, 73 (1952).

The solid line representing the differential cross section $d\sigma/d\Omega$ is subject to some error due to the inaccuracy introduced by averaging $\sin\theta$ over a 30° interval; but it is included to show the approximate half-width of the forward peak, which is estimated to be 25°. On the other hand, the $d\sigma/d\theta$ points are useful in comparing the relative forward to backward scattering; they show that the events under the peak constitute about one-half of the total dt cross section. Heidmann has pointed out[11] that the critical tests between theory and experiment are, in order of increasing sensitivity to large momentum changes (and thus small interaction distances): the total dt cross section, the angular half-width of fast forward deuterons, and the ratio of forward to backward deuterons. The following is a comparison between theory and experiment on these points:

	Theory	Experiment
Total σ_{dt}	16 mb	13±2.2 mb
Half-width	8.4°	~25°
Ratio forward/backward[14]	1000/1	1/1

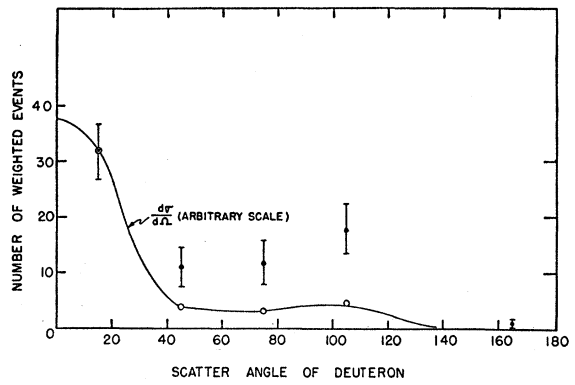

FIG. 9. Relative number of deuterons per unit scatter angle and per unit solid angle from dt events. The solid line connects points obtained from division by the average number of steradians in 30° scatter angle intervals.

The discrepancies increase exactly in the order listed above, with only the total σ_{dt} being in satisfactory agreement.

The one event plotted in the 165° group is a low energy deuteron with an associated triton going forward with 75 Mev. The process responsible for this is undoubtedly triton pick-up.

In Fig. 10 the energy distribution of the deuterons from dt events is plotted. The peak corresponding to pick-up deuterons falls at 50 Mev. Although the dt process is a two-body problem, there is no one-to-one correspondence between a point on the angular distribution plot and a point on the energy distribution plot because of the variety of energies of the incident neutrons. This fact, incidentally, must be kept in mind in making all comparisons with Heidmann's theory,

[14] Strictly, the experimental ratio observed is pick-up deuterons to non-pick-up deuterons.

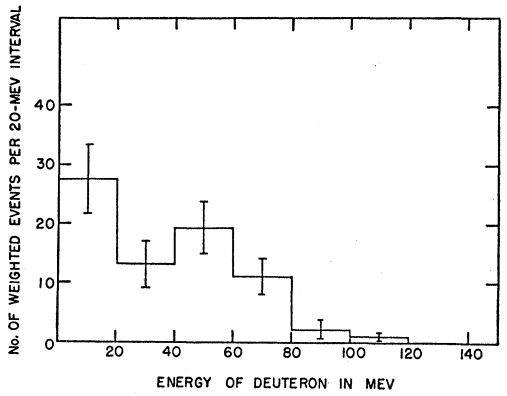

FIG. 10. Energy distribution of deuterons from dt events.

since he analyzed the problem for monochromatic 90-Mev incident neutrons.

The $He^4(n, pn)t$ *Reaction*

According to Heidmann's prediction the tritons from the pt reaction are of low energy (2 Mev on the average) and are distributed almost isotropically. Figure 11 shows the energy distribution of the tritons, and agreement is seen to be excellent. However, Fig. 12 shows that the angular distribution of the tritons is not isotropic but concentrated in the forward direction. The proton energy distribution is shown in Fig. 13.

The proton angular distribution from pt events is plotted in Fig. 14 together with the proton angular distribution from pd events. For both distributions it can be said that the free nucleon n-p scattering is reflected to some extent. This would be expected on the basis of a model first proposed by Serber,[15] developed in greater detail by Goldberger,[16] and whose general features were verified by Hadley and York.[1] According to this picture, the bombarding particle interacts with an individual nucleon rather than with the struck nucleus as a whole, and probably leading to the ejection of a fast particle in the forward direction.

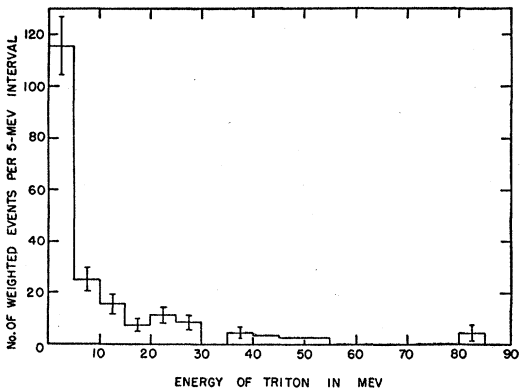

FIG. 11. Energy distribution of tritions from pt events.

[15] R. Serber, Phys. Rev. **72**, 1114 (1947).
[16] M. Goldberger, Phys. Rev. **74**, 1269 (1948).

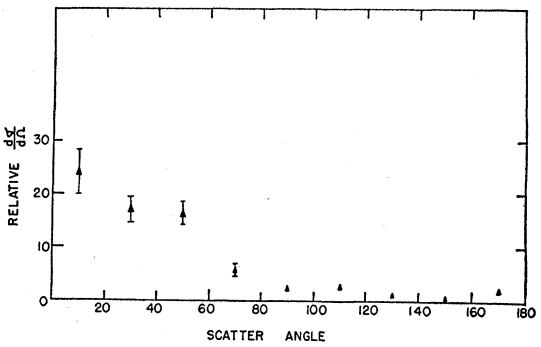

FIG. 12. Relative number of tritons per unit solid angle from *pt* events.

Figure 15 gives the energy distribution of protons from *pd* events. The statistics are not good because of the low frequency of occurrence of this type of event. Nor does any theory exist at present with which comparison can be made.

8. Experimental Checks

Stopping Power of Gas Mixture

A check was made of the range-energy relations expected from the calculated stopping power of the gas mixture in the chamber. The energies of a few long proton tracks ending in the chamber were determined from $H\rho$ measurements. The measured ranges agreed well within experimental error with the calculated ranges based on a stopping power of 0.185.

Oxygen Stars

From the partial pressures existing in the chamber immediately after expansion, the ratio of helium to oxygen nuclei was computed to be 51.8. If one assumes roughly that the ratio of inelastic events to total events (σ_i/σ_t) is the same for oxygen and helium, then the number of two-prong helium stars can be compared with the number of oxygen stars which show two or more prongs. The observed ratio is 12.2, and the ratio

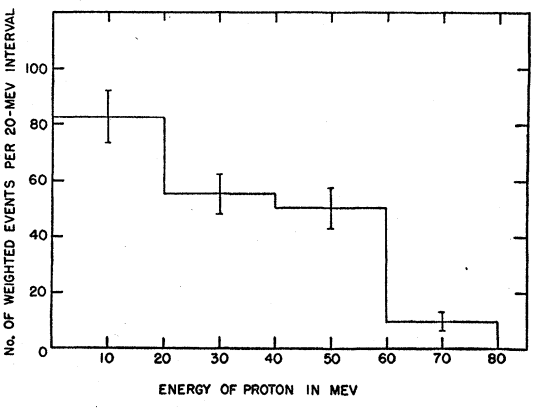

FIG. 13. Energy distribution of protons from *pt* events.

expected on the basis of the cross sections from reference 8 is 12.9.

Azimuthal Symmetry

One of the implied assumptions of this experiment is that all processes occur with azimuthal symmetry. This is borne out, within statistical errors, when He^4 recoils, and tritons from *pt* events, are compared in four azimuthal angle groups.

VI. CONCLUSIONS

When helium is bombarded by 90-Mev neutrons, the dominant process is elastic scattering, which exhibits the characteristic forward diffraction peak for incident neutron energies above 40 Mev. For neutron energies below 40 Mev, elastic scattering tends to become more isotropic. The most frequent inelastic process is the disintegration in which the incident neutron strips off a proton from the helium nucleus leaving a low energy

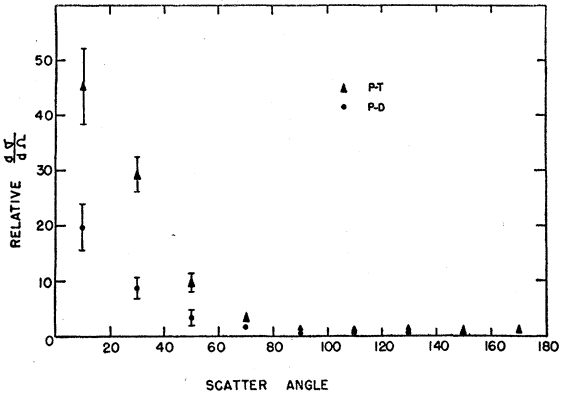

FIG. 14. Relative number of protons per unit solid angle from *pt* and *pd* events.

triton behind. A special case of this process occurs when the outgoing neutron and proton proceed together as a high energy forward deuteron—the so-called pick-up process. Pick-up accounts for about one-half of the events in which a deuteron and a triton are emitted; in the other half the deuteron comes off in a random direction with low energy. Although Heidmann's theory may be criticized in a number of ways, as pointed out by the author, it is in good agreement with the cross sections for elastic scattering and *pt* and *dt* disintegrations. The most serious discrepancies arise when the theoretical ratio of forward pick-up deuterons to backward deuterons of 1000/1 is compared with the experimental ratio of 1/1; also the theory predicts a much smaller number of *pd* and *dd* disintegrations than is observed. As far as the energy dependences are concerned, no sharp dependence is evident for elastic scattering (above 40 Mev) and for *pt* and *pd* disintegrations, while the *dt* disintegrations fall off with increasing energy, as is expected at least for the pick-up part of the process.

Noteworthy in the angular distributions is the fact that the proton angular distributions from *pt* and *pd* disintegrations reflect to some extent the free *n-p* interaction. Since He^3's could not be distinguished from He^4's in this investigation, the mechanism leading to He^3 production has been assumed to be similar to that leading to triton production. The possible errors arising from this assumption would seriously affect only the $He^4(n, 2n)He^3$ cross section.

Since at higher incident neutron energies, say 270 Mev, the theoretical approximation that the bombarding particle interacts only with one nucleon in the target nucleus becomes much better, the calculations become simplified, and hence neutron-helium scattering at this energy should prove to be of decisive interest. Further, the parallel experiment to the present one, namely proton-helium scattering at high energies would, together with the results of the present investigation, provide further comparison between the *n-n* and *n-p* and *p-p* forces.

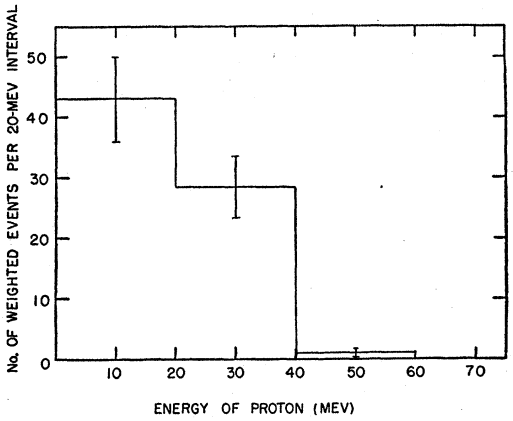

FIG. 15. Energy distribution of protons from *pd* events.

The author wishes to express his sincere gratitude to Professor Wilson Powell for suggesting this problem and for his helpful advice and constant encouragement throughout the investigation. The cooperation of many members of the cloud-chamber group is also acknowledged with pleasure, and special thanks are due to Dorothy Gardner for carrying out a large share of the calculations and to Beverly Lee who did the computation in the earlier stages.

APPENDIX I

In order to find the solid angle correction for a single prong event, one computes what fraction of the azimuthal angle ϕ (the angle between the projection of the initial track direction on a plane perpendicular to the neutron beam and the horizontal plane) meets the requirement at the given scatter angle θ that the dip angle α be less than $\pm 30°$.

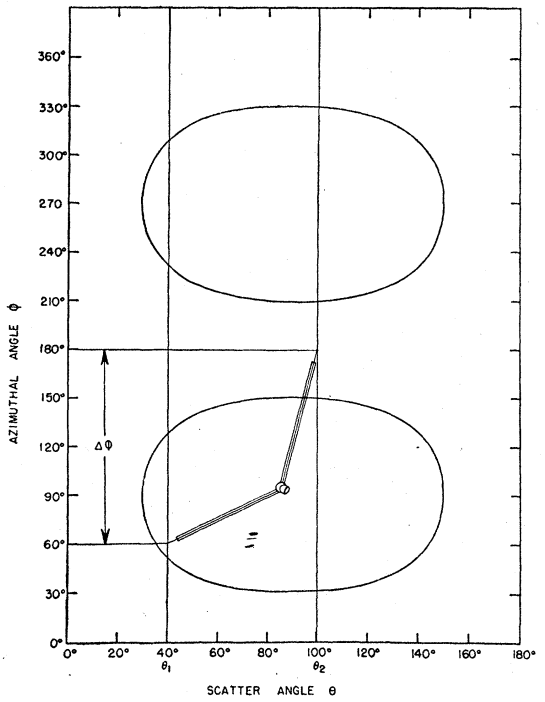

FIG. 16. Graph used for solid angle correction. Regions inside the ovals are excluded when dip angle α is restricted to the range from $+30°$ to $-30°$.

In Fig. 16 the direction in space of any track is given by a point in the $\phi-\theta$ plane; the oval regions are defined by the equation

$$\sin\phi = \sin\alpha/\sin\theta,$$

with $\sin\alpha = \pm\frac{1}{2}$. The interpretation of the plot is as follows: A track with a given scatter angle θ would be measured for those azimuthal angles ϕ which fall outside the oval regions. Consequently the probability of having observed a track when it has a given scatter angle θ is simply the ratio of the number of ϕ degrees outside the ovals to 360 degrees.

A two-prong event is geometrically defined by the three parameters θ_1 (prong 1), θ_2 (prong 2), and $\Delta\phi$ on the assumption of azimuthal symmetry. The correction factor is obtained graphically from Fig. 16 as follows: One leg of a pair of dividers is always kept on θ_1 while the other leg is always kept on θ_2. The angle between the legs is fixed by the parameter $\Delta\phi$. The dividers are then moved vertically up the plot so that θ_1 moves from $\phi=0°$ to $\phi=360°$. Everytime one or the other leg crosses into or out of the restricted regions the fact is recorded. From this information one can calculate two correction factors—one factor gives the number of events to be expected in the azimuthal region where one prong is too slanted; the other gives the number where both prongs are too slanted. The sum of the measured event and the two correction factors is the number of events which would have been observed if there had been no restriction on the dip angle α.

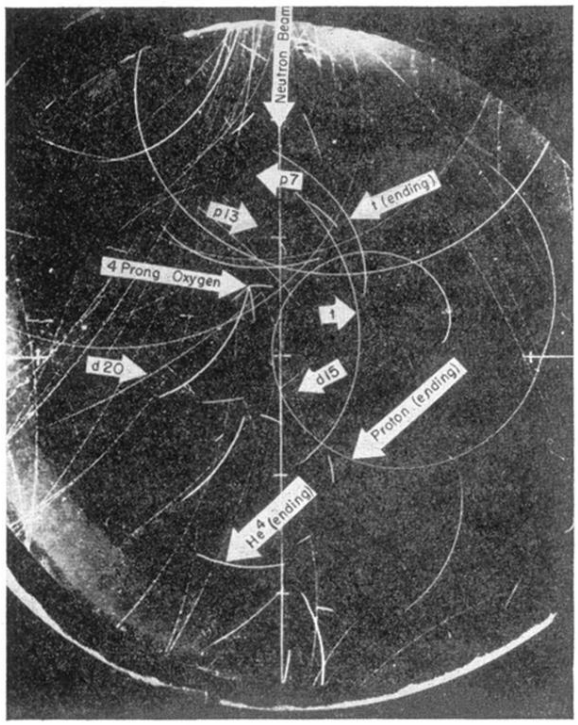

FIG. 3. Photograph showing examples of events that were analyzed. The letters are abbreviations for the particles and the numbers stand for the dE/dx values with respect to minimum ionization.

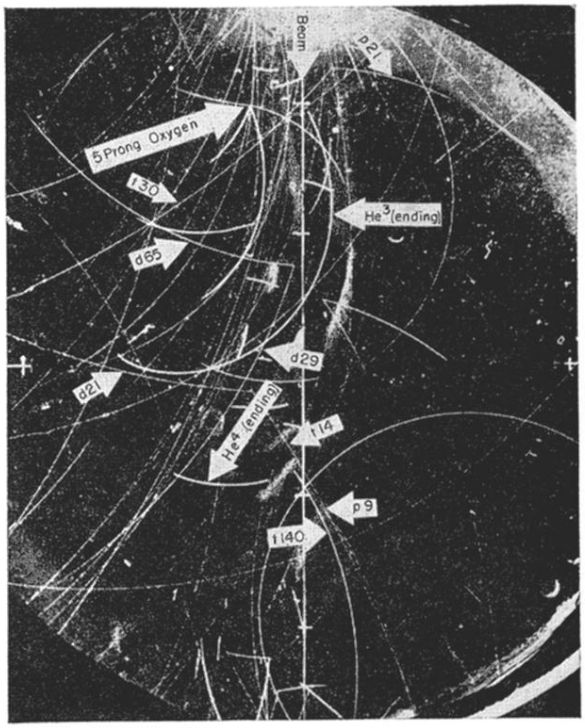

FIG. 4. Another sample picture. The lightest tracks which were dealt with are about 4–5 times with respect to minimum ionization and are only barely visible in the reproduction; the heaviest tracks encountered are as high as 400 times.